Available online at www.sciencedirect.com

ScienceDirect

Procedia Engineering 114 (2015) 215 – 222

Procedia Engineering

www.elsevier.com/locate/procedia

1st International Conference on Structural Integrity

2D and 3D Digital Image Correlation in Civil Engineering – Measurements in a Masonry Wall

Tiago Ramos[a]*, André Furtado[b], Shayan Eslami[a], Sofia Alves[a], Hugo Rodrigues[c], António Arêde[b] , Paulo J. Tavares[a], P. M. G. P. Moreira[a]

[a]*INEGI – Institute of Science and Innovation in Mechanical and Industrial Engineering, 4200-465 Porto, Portugal*
[b]*LESE – Laboratory for Earthquacke and Strucutral Engineering, 4200-465 Porto, Portugal*
[c]*RISCO-ESTG, Polytechnic Institute of Leiria, Portugal*

Abstract

Reinforced concrete structures play an important role in modern buildings, and common architectural designs often include RC frames strengthened with infill masonry panels. Due to their brittle nature, these components' failure and collapse have been subject of studies which can lead to proper structural diagnose and design in order to decrease their risk to human lives during seismic activities. Digital image correlation was used in two of these studies, in order to validate its ability for large specimens monitoring and future structural health monitoring applications. It enabled spatial reconstruction of the wall movement, characterization of its rigid body motion and measurement of both displacements and strain fields in in-plane and out-of-plane load applications. Data post-processing allowed the identification of common in-plane damages in the wall such as corner crushing and separation between infill and resistant structure.

Peer-review under responsibility of INEGI - Institute of Science and Innovation in Mechanical and Industrial Engineering

Keywords: Digital Image Correlation, DIC, Civil, Engineering, Masonry, Wall, Seism

1. Introduction

Reinforced concrete (RC) structures play an important role in modern buildings, and common architectural designs often include RC frames strengthened with infill masonry panels. Although the actual design codes consider the infill panels as non-structural elements, recent earthquakes showed that when subjected to horizontal cyclic

*Corresponding author. Tel.: +351–22–9578710; fax: +351–22–9537352.
E-mail address: tramos@inegi.up.pt

Peer-review under responsibility of INEGI - Institute of Science and Innovation in Mechanical and Industrial Engineering
doi:10.1016/j.proeng.2015.08.061

loadings the infill panels may change drastically the expected structural response of the building. In fact, an infill presence significantly reduces the natural period of the structure and consequently increases the expected seismic demand [1]. Furthermore due to their brittle nature, several infill damages or even collapses were observed in buildings subjected to earthquakes. Common damages in masonry enclosure walls, due to in-plane solicitation, often include [2]:

- Separation between infill and resistant structure
- Diagonal cracking
- Wall corner crushing

These damage types can condition and determine the failure and downfall behaviour of a wall during an out-of-plane solicitation.

Although the primary objective of the tests here described was to characterize the masonry infill walls behaviour when subjected to seismic loadings, digital image correlation was used in order to validate its ability for large specimens monitoring and future structural health monitoring (SHM) applications.

Digital Image Correlation (DIC) is a non-contact, full-field, optical technic to measure displacement fields in both in-plane (2D) or out-of-plane (3D) solicitations. It consists of recording images in different stages of a test, with dissimilar perspectives (if stereoscopy is required), dividing them in small sections, or subsets, and track their displacements along the different captured images. Despite the fact that this technique is commonly used with small test specimens, it can also be employed for large structures, being its accuracy essentially a function of the recorded images resolution.

The two distinct tests were performed with different objectives, loads and equipment setup. While the first consisted of an in-plane shear test in order to promote crack initiation and simulate seismic activity effects, the second was a quasi-static out-of-plane cyclic test in order to induce the wall downfall.

Lecompte [3], Küntz [4] and Destrebecq [5] had already used DIC to measure cracking processes and the flexural behaviour of concrete beams, but Salmanpour and Mojsivolic [6] or Ghorbani [7] had used this measurement technique in large (~4.5m^2) confined masonry walls in order to detect and trace accurate crack maps in a shear stress solicitation test. Nevertheless, this is, to the best of the writers' awareness, the first published study of 3D DIC measurements in both in-plane and out-of-plane solicitation tests.

Digital image correlation was used in order to spatially reconstruct the wall movement, characterize its rigid body motion and to measure displacements and strain fields in both two and three-dimensional load applications.

Fig. 1 shows two pictures from the wall for a scaling purpose. Possible curved fringes observed are not part of the applied pattern but an optical effect of the Moiré regular pattern in the camera sensor.

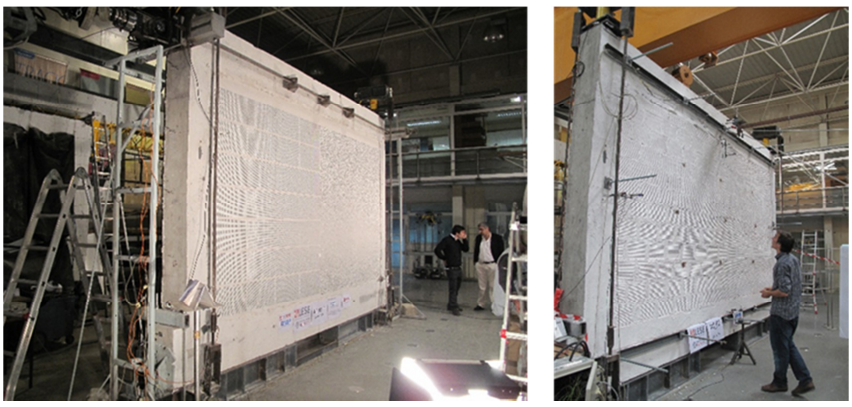

Fig. 1: Masonry wall, with applied regular and random patterns, for both tests.

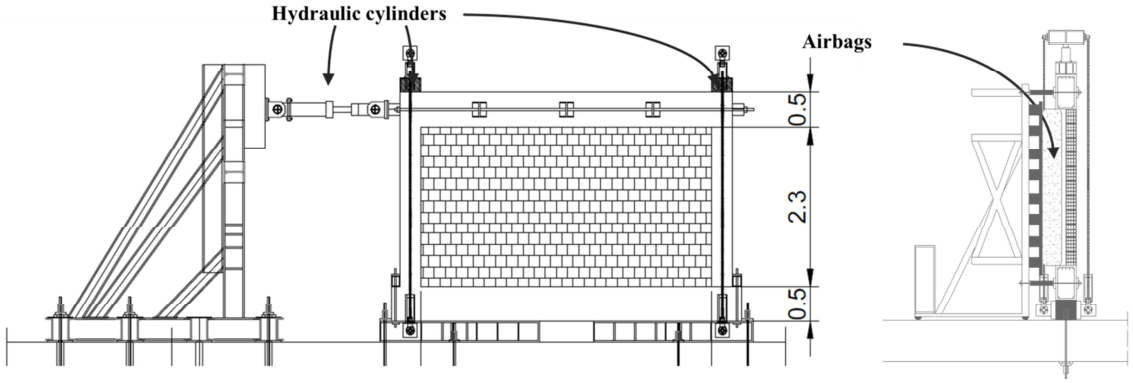

Fig. 2: Masonry wall dimensions and actuators setup for the in-plane test (front-view: (a)) and out-of-plane test (lateral-view: (b)).

2. Test Description and Equipment Setup

The tests were performed in a 4.22m × 2.30m (~9.66m^2) masonry wall with a RC frame as shown in Fig. 2(a). For the in-plane test, three hydraulic cylinders were used: two to compress the upper RC frame and another, placed horizontally, to generate the shear stress solicitation as shown in Fig. 2(a). For the quasi-static test, 8 airbags were positioned behind the wall. When pressurized, these devices compress the wall uniformly from the back, promoting its out-of-plane motion. Other tight rods and secondary structural elements were not represented in Fig. 2 and not mentioned in the paper since the author found its relevance, for the presented subject, minor. The wall was also equipped with several linear variable differential transformers (LVDT) around its RC frame for the in-plane test and perpendicularly to the masonry wall for the out-of plane test.

The DIC setup included the VIC-3D™ system from Correlated Solutions equipped with two 4.1MPixel CMOSIS cameras and two Schneider-Kreuznach 16mm focal distance lenses. For the in-plane experiment, only one camera was used, and the test was considered as a 2D analysis. For this test, image calibration was only necessary in order to reduce lenses distortion effects and to compute a scale measurement (from pixels to mm), while for the 3D measurements a customized 1.5m × 1.5m calibration pattern was produced in order to measure both intrinsic and extrinsic cameras parameters to enable a stereo surface reconstruction by the VIC-3D™ . The full equipment setup is presented in Fig. 3.

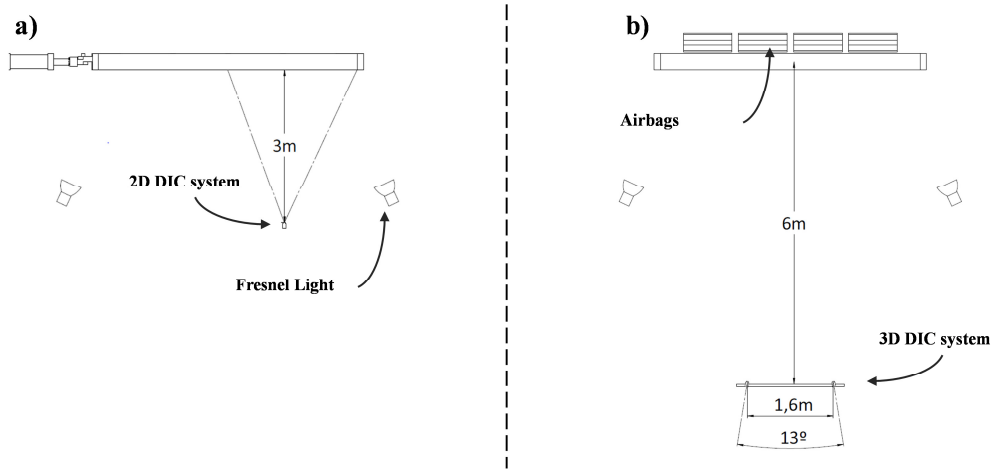

Fig. 3: Equipment setup for the in-plane (a) and out-of-plane (b) tests.

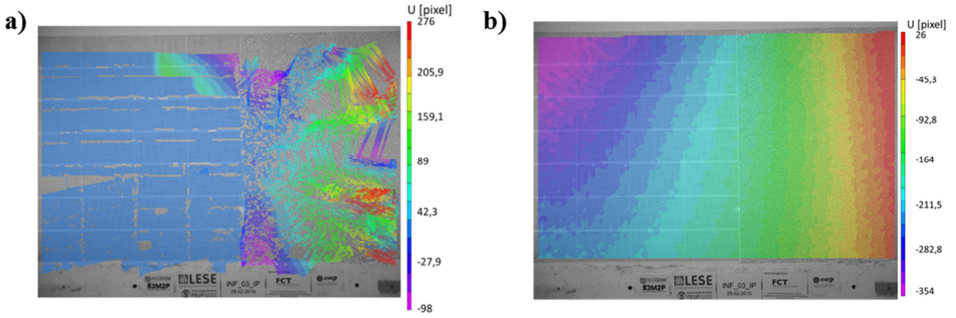

Fig. 4: Horizontal displacement field results with images from the secondary auxiliary camera for a random test step. Results with inappropriate (a) and correct (b) initial seed positioning.

Since another optical monitoring technique (Moiré fringe projection) was also used (for comparison research and to be published in another paper) the masonry wall was divided in two similar sections and two different patterns were applied: the Moiré periodic and regular pattern was applied on the left side of the wall and a random speckle pattern, for DIC application, applied on the right side. An auxiliary digital camera was placed in the center of the wall to evaluate the possibility extent to use periodic regular patterns with DIC algorithms.

Thereafter, the first monitored test (in-plane) only include accurate displacement and strain field measurements for the right side of the wall, although it was found by the research team, and with the use of the secondary auxiliary camera, that the VIC-3D™ software is capable of measuring small displacements in regular patterns if the initial seed is positioned in a random speckle pattern first. An example of this is presented in Fig. 4 for the horizontal displacement field in a random stage of the in-plane test. Defective results for initial seed position in the regular pattern are presented in Fig. 4(a) and accurate results when seed is positioned in the random speckle pattern are shown in Fig. 4(b). As a consequence of this optimistic result, for the out-of-plane test the whole wall was monitored, using DIC algorithms with both random and periodic patterns.

Regarding the applied patterns an alternative solution, to the ones commonly used by the DIC users' community is commonly being practiced by the present research group for large specimens. For the random speckle, after applying a white layer of ink over the monitoring target, a vinyl (polyvinyl chloride) stencil made of 4mm diameter (to assure a 3 to 8 image pixels per dot ratio) independent dots was transferred to the wall surface. The use of vinyl stencils presents itself as an alternative to the traditional ink solutions, since it is made from an "elastic" material, gives a good surface contrast, can be produced in large areas and can be applied in a single user's motion.

As mentioned before, the in-plane test was driven by a horizontal hydraulic cylinder, while the out-of-plane promoted by different airbags compression. Both the tests were carried out cyclically with gradually increasing applied loads as shown in Fig. 5. The total applied force by the airbags in Fig. 5(b) is a rough approximation calculated by the sum of the airbags internal pressure (measured) times their contact area with the wall.

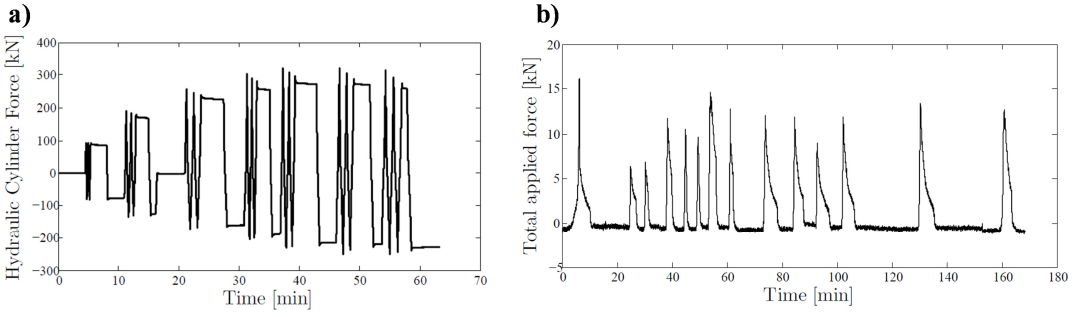

Fig. 5: Loads variations for the in-plane (a) and out-of-plane (b) tests over time.

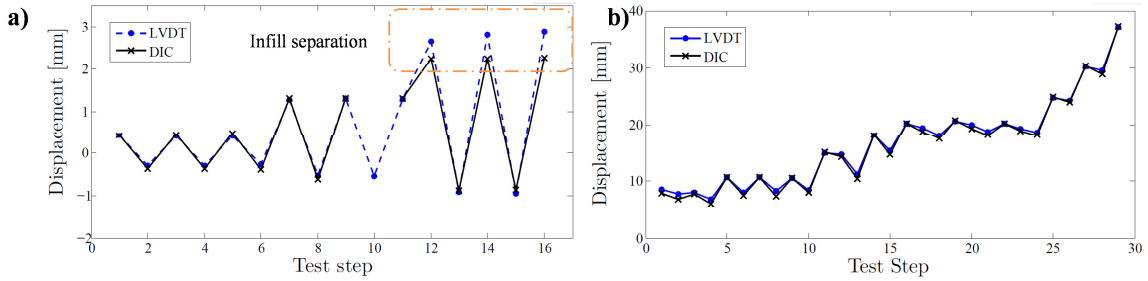

Fig. 6: LVDT and DIC results comparison for both in-plane (a) and out of plane (b) tests.

3. Data Processing and test Results

Since the DIC images were shot almost continuously during both tests, a large data sample was collected. In order to simplify the useful data analysis a first image processing procedure was done with large subsets and low spatial resolution. This allowed identifying the first 15 displacement peaks for the in-plane and the first 29 for the out-of-plane test. The corresponding images were after reanalysed with smaller subsets and higher resolution for more accurate results.

After identifying the corresponding displacement peak values for the LVDTs measurements, the results were compared with the DIC assessment. Fig. 6 shows an example of these comparisons for the in-plane (a) and out-of-plane (b) tests.

For the out-of-plane test the point in the centre of the wall was compared with an LVDT sensor overlapped exactly in the same region. On the other hand, for the in-plane test, due to the nature of the displacement field, the DIC results were compared with the LVDTs sensors in the RC frame by choosing the closest point adjacent to it inside the masonry wall.

It is noteworthy that for positive displacement values, in Fig. 6(a), the wall is being pushed by the hydraulic cylinder from left to right and the presented results correspond to a point close to the right RC frame of the wall. The differences between the two measurement techniques represented in this image may be explained by the infill separation from the RC frame. This is also supported by the fact that the larger differences occur for the steps corresponding to large tensile loads applied in the RC frame. On the other hand, since for steps 13 and 15 the right RC frame is being compressed along with the masonry wall (absence of infill separation) both the measurement data seem to agree.

The out-of-plane results comparison in Fig. 6(b) also showed a good correlation between both techniques, validating the DIC results for the whole displacement field evaluation.

Other post-processing operations were done in MATLAB®. In order to better display the determined displacement and strain fields, the data from the different steps from the in-plane test were imported, corrected, filtered and represented as shown in Fig. 9. Although low-pass filtering operations are already embed in VIC-3D™ data processing, in order to smooth the extracted fields, a Savitzky-Golay [8] digital filter was applied in both data directions with a third degree polynomial interpolation function. An example of this is represented in Fig. 7. Fig. 7(a) shows the first principle strain of the results for a random step chosen from the in-plane test. After applying the digital filter, as explained, the final result resembles the one in Fig. 7(b).

Despite this filtering operation may seem too aggressive to the signal and may attenuate some high magnitude values, the main objective of this operation was indeed to produce smooth strain fields to be used for vector illustrations as the one in Fig. 9(b), in order to produce clean and clear visual representations.

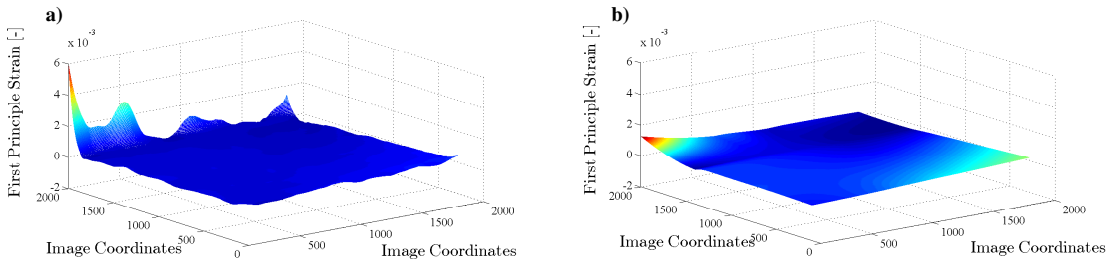

Fig. 7: First principle strain before (a) and after (b) applying the Savitsky-Golay digital filter.

To correct some ineffectiveness in the unwrapping operations, also performed by the VIC-3D™ software, a Fourier-base exact solution for deterministic phase unwrapping based in the Volkov and Zhu [9] algorithm was used. This procedure is faster than other commonly adopted unwrapping algorithms, and since is exact and non-dependant of a spatial path, it is inherently more accurate for the phase map corners even in the presence of noise.

One example of this operation can be observed in Fig. 8, where the peaks in Fig. 8(a) were corrected (or unwrapped) transforming this signal into the one in Fig. 8(b). This phase rectification was important for the correct and precise strain field representation as shown in Fig. 9(b).

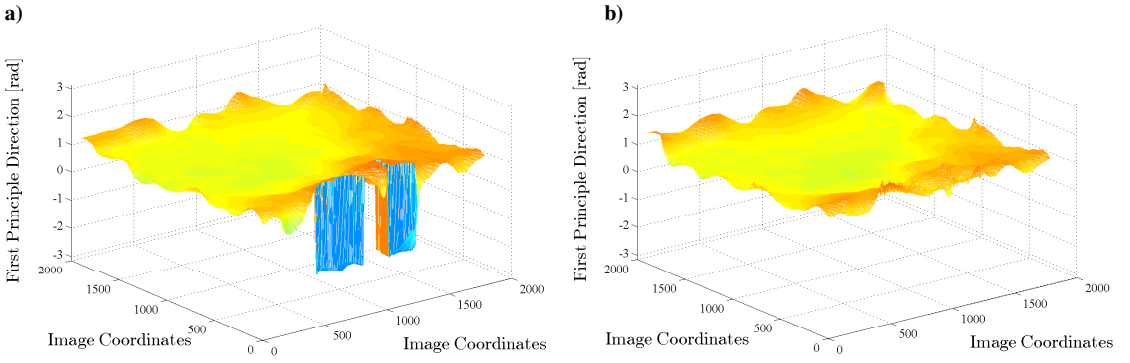

Fig. 8: Phase before (a) and after (b) unwrapping operation using the Volkov algorithm.

Fig. 9 shows a representation of the displacement field (a) and strain field (b) as a vector plot distribution over the right half of the masonry wall. For the strain field, centripetal vectors imply compression and centrifugal vectors tensile stress/strain. The vectors concern the principal strains and are oriented with the corresponding principal directions. As it can be seen, for a displacement field such as the one in Fig. 9(a), the right side of the masonry wall presented a uniform strain field mainly oriented along the wall diagonals. Above the main diagonal (*bottom-left* to *top-right*) it is possible to observe tensile strains in both principle directions, while below this diagonal, and in the other principal direction, compression prevails. This is especially important in the *bottom-right* corner of the wall where the high-magnitude compression vectors are inherent to the corner crushing damage, naturally frequent for in-plane solicitations. Fig. 9(c) shows a detail view of this phenomenon where it is clearly displayed the strong corner compression along the secondary diagonal (*top-left* to *bottom-right*).

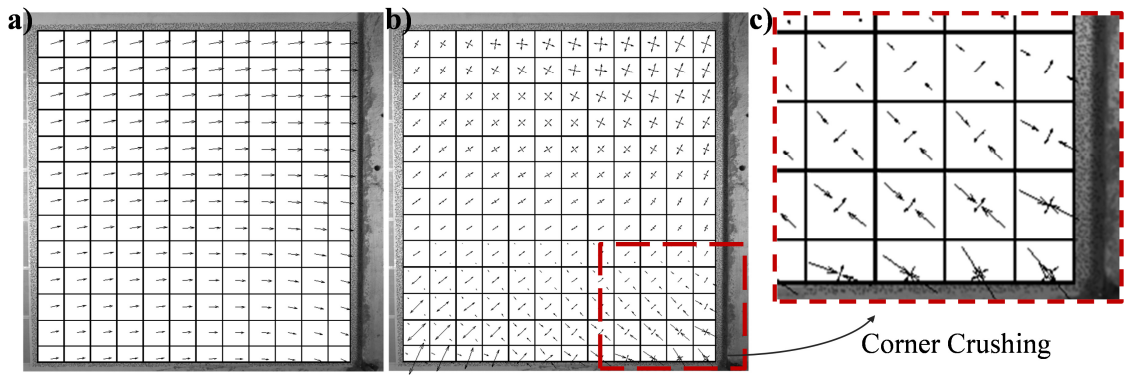

Fig. 9: Displacement field (a), strain field (b) and detailed view (c) for the right half of the wall, in the in-plane test (step15).

Fig. 10 shows a 3D spatial reconstruction of a polygonal shape made from representative points of the wall for the different selected steps and a real image from an external masonry wall downfall after an earthquake. The absence of significant strain fields for the out-of-plane test presupposes a rigid body motion behaviour. As in an earthquake, after an in-plane solicitation, shear stresses lead to cracks formation that tend to separate the masonry wall from the upper part of the RC frame. This event makes the upper part of the masonry wall the first section to fall, accelerating the whole wall collapse.

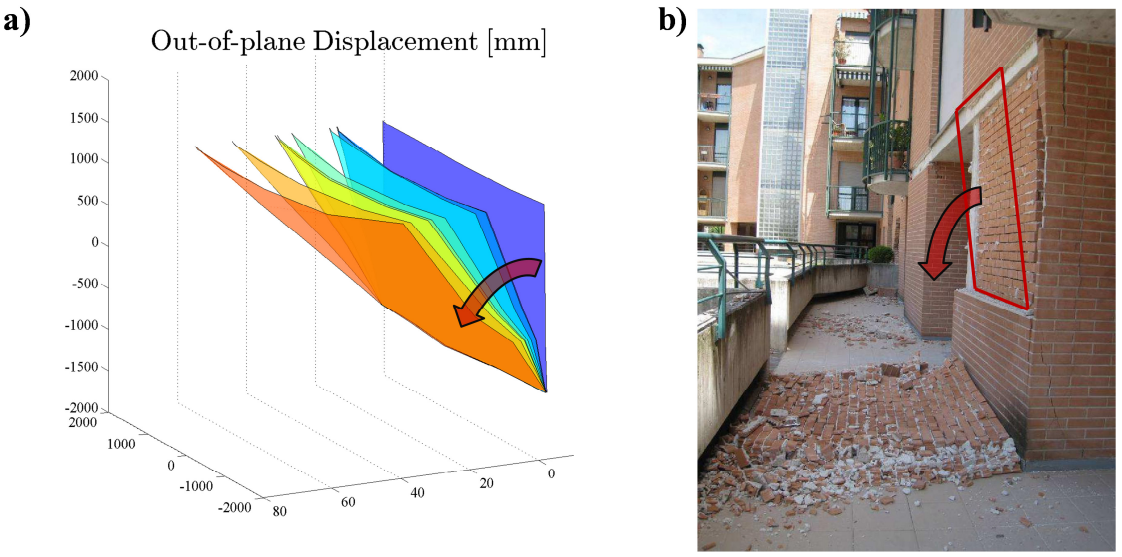

Fig. 10: (a) Simplified reconstruction of the out-of-plane tested wall failure; (b) Field evidence of a masonry enclosure wall failure.

4. Conclusions

Digital image correlation is a versatile optical technique which applications can be extended to structural health monitoring operations since their abilities are, in theory, scalable to any application size.

Although the precision and accuracy in DIC measurements can be modified by changing their image processing variables, and even though low-pass filters and data interpolations were applied to the measurements results, these seemed to strongly agree with the LVDTs evaluations. For this reason, both the displacement and the strain fields determined by this technique were considered valid, evincing its advantages for civil engineering applications.

The use of digital image correlation provides a full-field, almost continuous, measurement possibility that would be equivalent to install innumerous sensors in every spatial direction. Therefore, this could be an easier, low-priced and competitive monitoring technique to the ones already existing.

The main disadvantages of optic methods lie in the need of a controlled environment that may not be a possibility for all monitoring subjects. The presence of ground vibrations or other severe conditions may lead to a relative movement in the cameras that can influence the measured results or vary the initial camera calibration parameters which in turn invalidate the **computed** data.

For the in-plane test, both separation between the infill and the RC frame and corner crushing damages were identified and quantified. Diagonal cracking was not possible to examine only due to the plasterwork applied on the monitored side of the wall.

Acknowledgments

The authors gratefully acknowledge INEGI – Instituto de Ciência e Inovação em Engenharia Mecânica e Engenharia Industrial – for supporting the current work. Dr. Moreira acknowledges POPH (Programa Operacional Potencial Humano) QREN (Quadro de Referência Estratégico Nacional) - Tipologia 4.2 promotion of scientific employment funded by the ESF (European Social Fund) and MCTES (Ministério da Ciência, Tecnologia e Ensino Superior). The authors also acknowledge the support of FCT through project grant PTDC/EME-TME/120331/2010 – Combined Experimental-numerical methodology for SIF determination. This work was also developed within the frame of the Project Operação NORTE – 07 – 0124 – FEDER – 000009 - Applied Mechanics and Product Development, supported by SAESCTN-PIIC&DT/1/2011 programme, Novo Norte, QREN, to whom the financial support is to be acknowledged.

References

[1] H. R. H. V. A. C. a. J. M. S. R. Vicente, "Performance of masonry enclosure walls: lessons learned from recent earthquakes," Earthquake Engineering and Vibration, vol. 11, no. 1, pp. 23-34, 2012.

[2] C. C. A. A. a. H. R. André Furtado, "Geometric characterisation of Portuguese RC buildings with masonry infill walls," European Journal of Environmental and Civil Engineering, vol. In Press, 2015.

[3] J. V. H. S. D. Lecompte, "Crack Detection in a Concrete Beam using Two Different Camera Techniques," Structural Health Monitoring, vol. 5, no. 1, pp. 59-68, 2006.

[4] J. B. F. P. F. H. Michel Küntz Marc Jolin, "Digital image correlation analysis of crack behaviour in a reinforced concrete beam during a load test," Canadian Journal of Civil Engineering, vol. 33, no. 11, pp. 1418-1425, 2006.

[5] E. T. E. F. J. F. Destrebecq, "Analysis of Cracks and Deformations in a Full Scale Reinforce Concrete Beam using a Digital Image Correlation Technique," Experimental Mechanics, vol. 51, pp. 879-890, 2011.

[6] N. M. A. H. Salmanpour, "Application of Digital Image Correlation for strain measurements of large masonry walls," APCOM & ISCM, Zurich, 2013.

[7] F. M. M. A. S. R. Ghorbani, "Full-Field Deformation Measurement and Crack Mapping on Confined Masonry Walls Using Digital Image Correlation," Experimental Mechanics, vol. 55, pp. 227-243, 2014.

[8] M. J. E. G. Abraham Savitsky, "Smoothing and Differentiation of Data by Simplified Least Squares Procedures," Analytical Chemistry, vol. 36, no. 8, pp. 1627-1639, 1964.

[9] Y. Z. Vyacheslav V. Volkov, "Deterministic phase unwrapping in the presence of noise," Optic Letters, vol. 28, no. 22, 2003.